Feature-level Data Fusion and a Hybrid LSTM–Random-Forest Early-Warning Model for Deep-Ground-Pressure Prediction

Xuexiang Zhang[1], Hailong Zhang[1], Yajun Hu[1], Yude Liu[2,3], Xin Chen[1], Ning He[2,*]
[1]ShiCaoCun Colliery, Ningxia Coal Industry Co., Ltd, Ningxia, China
[2] North China Institute of Science & Technology, Langfang, China
3Beijing Yunmen Technology Co., Ltd, Beijing, China
E-mail: zhxxuem@163.com
*Corresponding author

Keywords: deep ground pressure, multi-source data fusion, Intelligent monitoring, LSTM neural network, random forest, early warning model

Received: August 21, 2025

To improve the level of mine safety protection, this study proposes a dynamic early warning model for deep mine pressure based on intelligent monitoring and multi-source data fusion. The study constructs a unified data fusion platform using multi-source heterogeneous data, including micro seismic monitoring, stress monitoring, ground temperature, hydrology, and mining progress. By combining the improved Long Short-Term Memory (LSTM) network with the Random Forest (RF) algorithm, a hybrid prediction model is established to realize the identification of mine pressure activity trends and the prediction of risk levels. The experiment adopts 12 months of monitoring data from a deep mine, which includes 8 feature channels from 6 types of sensors. The advance prediction time can reach 3 sampling cycles (approximately 1–3 hours). Compared with baseline models, the fusion model shows significant improvements. These baseline models include LSTM, Gated Recurrent Unit (GRU) network, RF, Support Vector Machine (SVM), and Logistic Regression (LR). On the test set, the fusion model achieves an accuracy of 86.7%±0.7%, a recall of 81.2%±0.7%, and an F1-score of 0.834±0.01. These metrics are significantly better than those of the single models. The experimental results show that the proposed fusion model can achieve more stable and reliable early warning in high-risk events, providing effective technical support for the safe production of deep mines.

Povzetek: Hibridni model LSTM-RF omogoča zanesljivo zgodnje opozarjanje na rudniški pritisk in povečuje varnost globokih rudnikov.

1 Introduction

With the development of the global economy and the increase in resource demand, mineral resources, as the foundation of national economic development, play a crucial role in modern society. However, with the gradual depletion of shallow mineral resources, the development of deep mineral resources has become an inevitable trend. At the same time, deep mine mining faces more complex geological environments and technical challenges. Especially in China, with the continuous growth of demand for energy, metals and other mineral resources, the excavation depth of deep mines has been increasing year by year. It increases the mining cost and brings more safety risks [1-3]. In the process of deep mine mining, mine pressure manifestation is a common phenomenon. Due to the huge ground stress on the deep rock strata and the influence of mining, the surrounding rock deforms and breaks, leading to a series of serious mine pressure problems, such as rock burst, rock burst and so on. These problems are characterized by strong suddenness and great harmfulness, which pose a great threat to the safe production of mines [4-6]. Therefore, how to effectively monitor and warn the deep mine pressure activities has become one of the key technical problems to be solved in the field of mining engineering. The traditional mine pressure monitoring methods mainly rely on the sensor data of single point or local area, such as the application of stress meter, displacement meter and other equipment. Although these traditional methods can reflect the mine pressure changes in a specific area to a certain extent, they can only provide local information and are difficult to comprehensively and accurately capture the dynamic change law of mine pressure in the whole mining area. Therefore, they have great limitations in practical application [7-9]. Traditional monitoring means usually lack the ability to process a large number of real-time data. It is difficult to realize the rapid response and accurate early warning of mine pressure disasters.

In recent years, the rapid development of emerging information technologies such as the Internet of Things, big data, cloud computing, and artificial intelligence (AI) has provided new solutions for deep mine pressure monitoring and early warning. By deploying various intelligent sensing devices, real-time monitoring of

multiple physical quantities (such as micro seismic signals, stress changes, groundwater levels, etc.) inside the mining area can be achieved, forming a massive multi-source heterogeneous dataset. Ge et al. also focused on using AI methods to optimize hydrate extraction strategies [10]. With the help of advanced data analysis algorithms, useful information can be mined from these complex data, providing a scientific basis for predicting mine pressure activity trends and evaluating potential risks [11, 12].

Against this backdrop, this study proposes an intelligent monitoring system based on multi-source data fusion and a corresponding deep mine pressure early warning model. The system integrates data obtained from various monitoring methods such as micro seismic monitoring, stress monitoring, ground temperature monitoring, and hydrological monitoring, and uses advanced data processing technologies and machine learning algorithms for comprehensive analysis. Compared with previous early warning methods that only rely on a single monitoring method (such as micro seismic or stress monitoring) or simple feature concatenation, this strategy can fully explore the potential correlation information between different data sources and improve the model's sensitivity and robustness to complex mine pressure changes. In terms of model structure, this study adopts a hybrid model combining Long Short-Term Memory (LSTM) network and Random Forest (RF). By integrating the temporal feature modeling capability of LSTM and the advantage of nonlinear classification of RF, high-precision prediction of abnormal mine pressure events is realized. Through ablation experiment analysis, it is found that the performance improvement mainly comes from the enhancement effect of the data fusion strategy at the key feature level. Meanwhile, the hybrid model structure can further improve the model's stability and response speed under complex geological conditions.

2 Recent work

In recent years, with the continuous deepening of deep mineral resource development, deep mine pressure monitoring technologies have attracted extensive attention and development. As an important means, micro seismic monitoring has been widely applied to real-time monitoring of rock mass fracture processes. According to the study by An and Mu, micro seismic monitoring can effectively capture energy release signals inside rocks, providing key data support for mine pressure activities [13]. Fuggi et al. pointed out that by optimizing the layout of micro seismic sensor networks and combining advanced signal processing algorithms, the positioning accuracy and identification efficiency of micro seismic events could be significantly improved, thereby enhancing the early warning capability for potential mine pressure disasters [14]. These studies highlight the importance of micro seismic monitoring in deep mine pressure early warning. They also indicate the limitations of solely relying on micro seismic data-such as the inability to comprehensively reflect changes in the stress field.

To overcome the limitations of single monitoring methods, multi-source data fusion has gradually become a research hotspot. Wei et al. proposed a method based on picture fuzzy sets, which effectively enhanced the decision-making ability in fuzzy and conflicting environments [15]. Their study indicated that in complex systems, improving information processing and feature fusion methods could enhance the accuracy and robustness of decision-making. The proposed mine pressure anomaly prediction also faced the challenges of multi-source features and uncertain information. Drawing on this idea, they improved the reliability and practicality of early warning through data fusion and a hybrid model structure. Similarly, Yuan et al. found that applying machine learning algorithms to the multi-source data fusion process not only improved data processing efficiency but also enhanced model prediction accuracy [16]. Habib et al. emphasized the importance of data standardization and feature selection, believing that reasonable data preprocessing steps were one of the key factors to ensure the effect of subsequent modeling [17]. The above studies show that by rationally using different types of monitoring data, the mine pressure status and its development trend can be evaluated more comprehensively and accurately.

The development of intelligent early warning models has provided new insights into deep mine pressure prediction. Demiss and Elsaigh introduced deep learning techniques into the field of mine pressure early warning, proposing a hybrid model combining Convolutional Neural Network (CNN) and LSTM, which demonstrated excellent performance in time series prediction [18]. Meanwhile, Kahraman et al. explored the application potential of ensemble learning methods in mine pressure prediction. The results showed that the RF algorithm performed well under complex geological conditions due to its strong nonlinear fitting ability and good robustness [19].

In the field of complex dynamic system control, a variety of adaptive control methods have been proposed in existing studies to address issues of system uncertainty and nonlinearity. Boulkroune et al. proposed an adaptive fuzzy control method that could achieve fixed-time synchronization of fractional-order chaotic systems in a short period, demonstrating high robustness. However, this method mainly focused on system state synchronization and did not involve issues related to multi-source data fusion and time-series prediction [20]. Bey 和 Chemachema 针对具有输入饱和、外部扰动及状态不可测的严格反馈多输入多输出非线性大系统，提出基于事件触发机制的自适应分散神经网络控制策略，通过控制误差替代跟踪误差简化自适应律推导，并利用模糊推理系统估计未知控制误差。然而，该方法主要关注控制系统本身的稳定性与精度，未涉及多源异构数据的融合处理，也缺乏对时序预测与实时预警场景的扩展支持 [21]. The nonlinear optimal control method for gas compressors proposed by Rigatos et al. optimized the dynamic response and steady-state performance of industrial drive systems, but it also failed to integrate multi-source heterogeneous data or address real-time early warning scenarios [22]. Table 1 summarizes the comparison of relevant literature,

including dataset types, methods, and evaluation indicators, and points out the limitations of each method:

Table 1: Literature comparison

Literature	Data type/scale	Method	Evaluating indicator	Limitation
An & Mu [13]	Micro seismic monitoring	Data driven	Energy release and capture ability	A single data source cannot reflect the change of stress field.
Fuggi et al. [14]	Micro seismic monitoring	Sensor optimization +signal processing	Positioning accuracy and identification efficiency	Lack of feature fusion and hybrid modeling
Wei [15]	Multi-attribute decision making	Picture Fuzzy method	Decision accuracy	Failure to combine time series prediction with dynamic events
Demiss & Elsaigh [18]	Historical ground pressure data	CNN-LSTM mixed model	Prediction accuracy	Single feature type, untreated multi-source fusion
Kahraman et al. [19]	Multi-source ground pressure data	RF integrated learning	Accuracy and robustness	Mixed modeling without combining time series and static features
Boulkroune et al. [20]	Nonlinear dynamic system	Adaptive fuzzy control	Robustness	Unprocessed multi-source sensor data and prediction
Bey 和 Chemachema [21]	多变量动态系统	神经自适应控制	控制精度与稳定性	未实现多源数据融合与实时预警
Rigatos et al. [22]	Industrial drive system	Nonlinear optimal control	Dynamic response and steady-state performance	Lack of real-time early warning and multi-source heterogeneous data processing

Comprehensively speaking, most existing studies lack feature-level fusion of heterogeneous monitoring data (such as micro seismic, stress, hydrological, and geological indicators). They rarely explore hybrid modeling ideas that combine temporal features with static environmental features, and most are only verified on small-scale or synthetic datasets, lacking systematic evaluation on real mine data. In addition, existing studies generally lack ablation experiments to distinguish the respective contributions of data fusion strategies and modeling structures. To address the above issues, the proposed LSTM-RF fusion early warning model achieves feature-level fusion by combining time-series features and static environmental features. It can fully utilize multi-source heterogeneous data, improve the accuracy, stability, and response speed of mine pressure anomaly prediction, and make up for the deficiencies of existing methods in multi-source data fusion and real-time early warning.

3 Method

3.1 Data acquisition and preprocessing

The dataset used in this study is derived from the intelligent monitoring system of a typical deep mine in China, covering multi-source heterogeneous data such as micro seismic monitoring, stress monitoring, ground temperature, hydrology, and mining progress. Specifically, 12 micro seismic sensors are deployed with an average sampling frequency of 50 Hz. 8 stress sensors are used, with a sampling frequency of 1 Hz. 6 ground temperature sensors are installed, with a sampling frequency of 0.1 Hz. 4 water level sensors are arranged, with a sampling frequency of 0.05 Hz. 2 Propulsion Progress Sensors are adopted, with a sampling frequency of 1 Hz. The data collection time spans from 2023 to 2024. After cleaning and screening, a total of approximately 36,000 samples is obtained, with 1,280 annotated mine pressure abnormal events. Among them, the sampling frequency of micro seismic and stress sensors is once every 10 minutes, the sampling frequency of ground temperature and hydrological data is once per hour, and the mining progress information is updated daily. The dataset is divided into a training set, a validation set, and a test set in chronological order, with the proportions of 70%, 15%, and 15% respectively.

The labels are determined based on the mine's historical early warning records and the annotation results of the monitoring system. A label value of 0 indicates that no early warning is triggered, while a value of 1 indicates that an early warning is triggered. The early warning labels are the result of comprehensive threshold judgment based

on multi-source data fusion combined with expert annotations. First, reasonable thresholds are set for key indicators such as cumulative micro seismic energy, stress gradient change, ground temperature change rate, water level change trend, and mining progress. For example, cumulative micro seismic energy exceeding the mean value plus 2 times the standard deviation is regarded as abnormal. These thresholds are jointly determined by the statistics of historical mine pressure event data and the experience of mine safety experts. Subsequently, manual review is conducted on the initially triggered abnormal points to eliminate noise data and misjudged points, and the final event time window is annotated. This ensures that each triggered Label=1 truly corresponds to a potential mine pressure abnormal event. This method combining threshold judgment and expert review not only ensures the objectivity of labels but also takes into account the safety sensitivity in actual mine scenarios. Early warning samples (label = 1) account for approximately 18%, while non-early warning samples (label = 0) account for approximately 82%. Data of each modality undergoes time alignment and standardization in the preprocessing stage to ensure the consistency and fusibility of data with different sampling frequencies.

In mining environments, data sources are extensive and diverse, mainly including micro seismic monitoring, stress changes, ground temperature variations, groundwater pressure, and working face advancement speed. These data reflect the changes of different physical quantities within the mining area and serve as important bases for mine pressure analysis. First, a complete monitoring system needs to be established to ensure real-time acquisition of high-quality data. For micro seismic monitoring, a high-sensitivity sensor network is adopted to capture energy signals released during rock mass fracture. For stress changes, stress meters installed on roadway walls or goafs are used for measurement. Ground temperature and hydrological data are obtained through temperature sensors and water level gauges, respectively. In addition, relevant parameters of mining activities, such as working face advancement speed and mining layout information, also need to be recorded.

Data preprocessing is the basis of follow-up analysis, which mainly includes missing value filling, outlier elimination, standardization and normalization, feature extraction and other steps. Suppose there is a dataset $D = \{x_1, x_2, ..., x_n\}$ containing n samples, in which each sample x_i is an M-dimensional vector, representing the values of various monitoring indicators at the ith moment. For the problem of missing values, the mean filling method or interpolation method can be used to deal with it. In the experiment, linear interpolation is mainly used for continuous time-series data such as micro seismic and stress data. While mean imputation is adopted for relatively stable data including ground temperature, hydrology, and mining progress. If a variable has a missing value, its filled value can be expressed as:

$$\hat{x}_j = \frac{\sum_{i=1}^{n} x_{ij}}{n}, j \in M \quad (1)$$

M is the index set where the missing value is located. $\hat{x}_j$ represents the padded value. x_{ij} represents the j-th eigenvalue of the i-th sample (time point or observation example), and n represents the number of samples. For outlier detection, this study uses the Z-Score method based on statistics. If the Z score of a sample point exceeds a certain threshold, it is considered as an outlier:

$$Z_j = \frac{x_j - \mu}{\sigma} \quad (2)$$

μ and σ are the sample mean and standard deviation respectively. The next step is to standardize the data so that all variables have the same scale range, which is convenient for subsequent modeling. The commonly used standardization methods are Min-Max scaling and Z-Score standardization. Min-Max scaling equation is as follows:

$$x_j' = \frac{x_j - min(X)}{max(X) - min(X)} \quad (3)$$

$min(X)$ and $max(X)$ are the minimum and maximum values in the sample set, respectively.

Finally, the feature engineering stage, through the transformation of the original data, extract new features that are more helpful to predict the task. The trend change can be reflected by calculating the difference between adjacent time points:

$$\Delta x_t = x_t - x_{t-1} \quad (4)$$

Δx_t represents the rate of change between two adjacent points.

3.2 Data Fusion Strategy

In the deep mine pressure monitoring and early warning system, sensor data from a single source often fails to comprehensively reflect the complex geological environment changes in the mining area. Due to the complex conditions of high ground stress, high temperature, and high osmotic pressure in deep mines, ground pressure events are characterized by strong suddenness, fast evolution, and multiple influencing factors. Relying solely on one or several independent data sources is prone to problems such as one-sided information, high misjudgment rates, and delayed early warnings. Therefore, constructing an efficient, stable, and robust mine pressure early warning model must rely on the effective fusion of multi-source heterogeneous data. Data fusion refers to the comprehensive processing of information from multiple different sensors or data sources to obtain more accurate and comprehensive environmental perception capabilities than a single data source. This technology is widely used in military reconnaissance, intelligent transportation, environmental monitoring, and other fields, achieving remarkable results. According to different fusion levels, data fusion can be divided into signal-level fusion, feature-level fusion, and decision-level fusion. Among them, feature-level fusion has become the mainstream method adopted by most intelligent prediction systems, as it reduces data

dimensions while preserving key information. The framework of the multi-source data fusion strategy is shown in Figure 1:

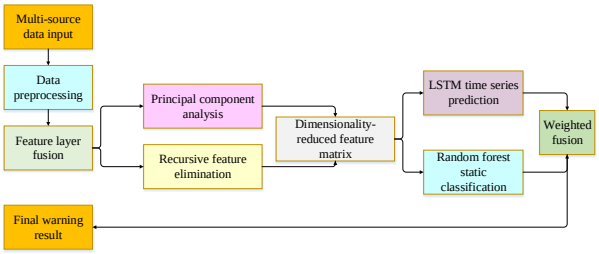

Figure 1: Multi-source data fusion strategy framework

In this study, a feature-level fusion strategy is adopted to conduct unified modeling and feature extraction on the multi-dimensional feature vectors of multi-source heterogeneous data, including preprocessed micro seismic energy, stress change, ground temperature, hydrology, and mining progress. Specifically, principal component analysis is first used to reduce the dimension of the original feature space, removing redundant information while preserving the main change trends. Subsequently, combined with the recursive feature elimination method, the most representative feature subsets for mine pressure state changes are screened to form the final input feature matrix. In the Principal Component Analysis (PCA) stage, a Cumulative Variance Contribution Ratio of 95% is retained to ensure that most information is preserved while reducing redundancy. In the Recursive Feature Elimination (RFE) stage, 5-fold Cross-Validation (5-CV) is used to determine the number of features in the optimal feature subset. Finally, 20 of the most representative features are selected as the model input. Table 2 lists some of the main finally selected features and their intuitive meanings, including cumulative micro seismic energy, stress gradient change, ground temperature change rate, water level change trend, and mining progress. These features intuitively reflect the correlation between each feature and the change of mine pressure state. This fusion approach not only improves data usability but also effectively enhances the model's generalization ability and stability.

Table 2: Some features of finally selected mine pressure prediction and its intuitive meaning

Feature number	Feature name	Feature type	Intuitive meaning/explanation
F1	Micro seismic energy accumulation	Dynamic characteristics	Reflect the total amount of energy released by rock mass fracture and predict the possibility of rock pressure activity
F2	Frequency of micro seismic events	Dynamic characteristics	The change of the number of micro seismic events per unit time is used to monitor the stress release trend.
F3	Stress gradient change	Dynamic characteristics	Reflect the stress change rate of roadway or goaf
F4	Geothermal change rate	Dynamic characteristics	Monitor the rising trend of deep mine temperature and reflect the thermal stress change of rock mass.
F5	Trend of water level change	Dynamic characteristics	Monitoring the change of groundwater pressure in mining area
F6	Mining progress	Static characteristics	Advance rate and cumulative advance distance of working face
F7	Rock dip angle	Static characteristics	Geometrical structure information of rock stratum affects stress distribution.
F8	Number of historical events of ground pressure	Static characteristics	The number and frequency of historical ground pressure events reflect high-risk areas.

In the subsequent modeling stage, the output of the LSTM network is treated as a dynamic feature and combined with other static features to form the input of the RF model. This approach belongs to feature-level early fusion, rather than weighted fusion at the model output stage. By integrating dynamic LSTM features with static features, the model can simultaneously capture temporal evolution patterns and static environmental information, thereby improving generalization, stability, and prediction accuracy. Through this feature-level fusion mechanism, the system achieves more accurate and timely mine pressure warnings in complex deep mining environments.

The LSTM network is a special type of Recurrent Neural Network (RNN), particularly suitable for handling long-term dependency problems [23]. When processing sequential information, standard RNN can capture temporal dependencies, but due to structural limitations, they struggle to effectively transmit and retain early information over long time intervals, making it difficult for the model to learn distant dependencies. LSTM addresses this challenge by introducing a structure called the "memory cell" and three gating mechanisms-input gate, forget gate, and output gate-to achieve selective retention and update of information. The core advantage

of LSTM lies in its ability to automatically determine which information needs long-term retention and which can be ignored or discarded. For example, the forget gate controls how much information from the previous state is passed to the current state, the input gate decides how new information at the current moment is written into the memory cell, and the output gate regulates how the content of the memory cell influences the current output. This mechanism enables LSTM to better capture long-term dependency features in time series during network training, making it suitable for modeling complex systems with temporal characteristics and dynamic patterns, such as the evolution process of mine pressure. Therefore, LSTM is widely applied in various fields like speech recognition, natural language processing, financial prediction, and industrial monitoring, especially for tasks requiring high-precision modeling and prediction of time series.

The input gate, forgetting gate and output gate of the LSTM unit are specifically represented as: let the forget gate be f_t , the input gate be i_t and the output gate be o_t , and their states are shown in the following equation:

$$f_t = \sigma(W_f \cdot [h_{t-1}, x_t] + b_f) \tag{5}$$

$$i_t = \sigma(W_i \cdot [h_{t-1}, x_t] + b_i) \tag{6}$$

$$o_t = \sigma(W_o \cdot [h_{t-1}, x_t] + b_o) \tag{7}$$

W is the weight matrix. h_{t-1} is the state of the hidden layer at the last moment. x_t is the current input, and b is the offset term. The cell status update is shown in the following equation:

$$C_t = f_t * C_{t-1} + i_t * tanh(W_C \cdot [h_{t-1}, x_t] + b_C) \tag{8}$$

$tanh$ is a hyperbolic tangent activation function.

The final hidden layer state is shown in the following equation:

$$h_t = o_t * tanh(C_t) \tag{9}$$

Next is the RF, an ensemble learning method that improves prediction accuracy by constructing multiple decision trees and aggregating their results [24]. Each tree is independently trained on a subset of the training set, and only a random subset of features is considered when splitting nodes each time. Suppose there are a total of T trees, the final prediction result can be obtained through a voting mechanism:

$$y = mode(y_1, y_2, ..., y_T) \tag{10}$$

y is the final prediction result, and $mode$ represents the mode operation.

The core idea of RF is to form a "forest" by constructing a large number of decision trees and leverage the collective wisdom of these trees for final classification or regression tasks [25]. Each decision tree is generated based on Bootstrap sampling (i.e., random sampling with replacement) to create a new training sample set from the original dataset. This means each tree "sees" a slightly different data distribution, thereby enhancing model diversity. When splitting nodes, RF not only performs random sampling on data samples but also randomly selects features.

RF aggregates the prediction results of individual trees through a voting mechanism (for classification problems) or averaging (for regression problems). In classification tasks, after each tree classifies the test samples, all classification results are summarized, and the category with the highest frequency is chosen as the final prediction. This approach not only improves the prediction accuracy of a single decision tree but also reduces overall errors caused by misclassification of individual trees. For regression tasks, RF uses simple averaging or weighted averaging to synthesize the predicted values of all trees for the final result. Studies have shown that RF performs excellently in handling high-dimensional data, nonlinear relationships, and scenarios with significant noise, making it particularly suitable for data analysis tasks in complex environments.

In practical applications, the advantages of RF can only be maximized by reasonably selecting and configuring its parameters in combination with the characteristics of specific application scenarios. By combining it with other advanced algorithms (such as LSTM), the prediction ability and application scope of the model can be further enhanced, providing new ideas and methods for solving complex problems.

3.3 Early warning model construction

Based on the above theoretical basis, the concrete construction process of the early warning model is described in detail below. First, for the design of the input layer of the LSTM model, considering the characteristics of multi-source heterogeneous data, it is necessary to map different types of data into the same dimension space. Assuming that there are k different monitoring data sources, a transformation matrix A_k can be defined to achieve this goal:

$$X' = A_k X \tag{11}$$

X represents input data, X' represents the converted unified format input data, and A_k is the conversion matrix.

Next, the transformed data is fed into the LSTM network for training, with the optimization goal of minimizing the Sum of Squared Errors (SSE), as shown in the following equation. Although the model aims at binary classification (warning/non-warning), the output of the LSTM network is treated as a continuous risk score and combined with the RF for final classification. Therefore, in the LSTM stage, SSE is used as a regression loss function for continuous outputs, which better fits the dynamic changes of risk trends and provides rich dynamic feature information for the subsequent RF. At the same time, to ensure the effectiveness of the binary classification task, the RF model adopts a traditional classification method (majority voting mechanism) for final label prediction, thereby achieving accurate warning determination.

$$SSE = \sum_{i=1}^{n} (y_i - \hat{y}_i)^2 \quad (12)$$

y_i is the real label. $\hat{y}_i$ is the predicted value of the model. To prevent over-fitting, a regularization term is added to the loss function, as shown in the following equation:

$$L = SSE + \lambda \|W\|^2 \quad (13)$$

λ is the regularization coefficient and W is the weight parameter in the network.

In the specific implementation process, to improve the generalization ability of LSTM under complex mining monitoring data, this study introduces improvement mechanisms based on the standard LSTM structure. First, a Dropout layer is added between the hidden layers of LSTM. It randomly discards part of the neurons to reduce strong dependencies among them, thereby effectively alleviating overfitting. Second, an L2 regularization constraint is applied during the optimization of network parameters. It penalizes the weight parameters to prevent the model from relying excessively on a small number of features. These improvements enable the model to maintain strong learning ability while achieving higher robustness and stability, making it more adaptable to the characteristics of multi-source heterogeneous monitoring data in deep mining environments.

After the training of LSTM model is completed, its output is taken as one of the features, and it is input into the RF model together with other features that have not participated in LSTM training. In practical scenarios of deep mine pressure monitoring, different decision trees show varying abilities in identifying high-risk (minority class) samples. To enhance the recognition of critical minority classes while maintaining overall prediction accuracy, a weighting mechanism based on the cross-validation accuracy of each tree is introduced at the RF output stage. Trees with better performance receive higher weights in the final prediction, thereby improving the sensitivity and stability in detecting mine pressure anomalies. This weighting strategy has already been applied in the study of Liu et al. [26]. Suppose there are T decision trees in the RF, and the prediction result of each tree is recorded as y_t, then the final warning level Y can be obtained by weighted average:

$$Y = \sum_{t=1}^{T} w_t y_t \quad (14)$$

w_t is the weight of each tree, which satisfies $\sum_{t=1}^{T} w_t = 1$. The weight of each tree is calculated based on its classification accuracy on the training set using five-fold cross-validation (5-fold Cross-Validation, 5-CV). Trees with higher accuracy receive larger weights, as shown in equation (15). During the real-time inference stage, these weights are fixed and not updated online. In this way, weighted averaging can comprehensively account for the predictive ability of each tree, thereby improving the stability and accuracy of the final warning results.

$$w_t = \frac{acc_t}{\sum_{t=1}^{T} acc_t} \quad (15)$$

acc_t is the accuracy of the t tree. This reasoning process is represented by pseudo code as shown in Figure 2:

```
Input: Multi-source raw data (micro-seismic, stress, temperature, hydrology, mining progress)
Output: Early warning alarm level

1: Data ingestion
  - Collect real-time sensor readings
2: Preprocessing
  - Handle missing values (mean fill / interpolation)
  - Outlier detection and removal
  - Standardization / normalization
  - Feature extraction (dynamic & static features)
3: LSTM inference window
  - Feed sequence of dynamic features into trained LSTM
  - Obtain LSTM output as dynamic feature vector
4: RF classification
  - Combine LSTM output with static features
  - Input to trained RF model
  - Obtain per-tree predictions
5: Weighted fusion
  - Apply precomputed tree weights to aggregate predictions (Eq. 14–15)
  - Compute final probability or warning score
6: Alarm thresholding
  - Compare warning score against predefined thresholds
  - Trigger alarm if score exceeds threshold
```

Figure 2: Real-time reasoning process pseudocode

The original output of the proposed model is a binary classification result (0 indicates no anomaly, and 1 indicates a mine pressure anomaly). For practical application and mine safety management, the prediction results are further mapped into three risk levels: low risk (Low), medium risk (Medium), and high risk (High). Low risk refers to samples with prediction probabilities below 0.33, indicating that the mine pressure state is basically normal and the short-term likelihood of anomalies is low. Medium risk refers to probabilities between 0.33 and 0.66, suggesting that there is a certain abnormal trend in mine pressure that requires attention. High risk refers to probabilities above 0.66, indicating a high likelihood of mine pressure anomalies, for which preventive measures should be taken promptly. The probability values are derived from the integrated risk scores produced by the fusion of LSTM and RF outputs, mapped to the [0,1] interval after weighted fusion, and then categorized according to the thresholds. This approach essentially uses probability outputs of the binary classification model for threshold-based grading, rather than multi-class training, thereby ensuring simplicity in model training and deployment while providing more intuitive risk references.

In the actual implementation, the hyperparameters of the model are explicitly specified to facilitate reproducibility. The details are shown in Table 3. The experiments are conducted on a workstation equipped with an NVIDIA RTX 3090 GPU, an AMD Ryzen 9 5950X CPU, and 128 GB of memory. A single training of the LSTM model takes about 45 minutes, while the RF model requires about 10 minutes. The fusion model introduces almost no additional overhead during the inference stage.

Table 3: Hyperparameter setting

Models	Structural setting	Key parameter	Optimizer/criterion
LSTM	Two-layer structure, 128 hidden cells in each layer, activation function tanh.	The learning rate is 0.001, the batch size is 64, the number of iterations is 100, and the Dropout ratio is 0.3.	Adam
RF	100 trees, with a maximum tree depth of 15.	Feature subset size = √ (total feature number), splitting criterion Gini index	CART (based on Gini)
Hybrid model (LSTM+RF)	Combining the results of LSTM and RF, through the weighted voting mechanism	Keep their respective hyperparameters unchanged, and the voting weight is adjusted based on the verification set.	Adam + Gini

To sum up, the early warning model construction framework is shown in Figure 3 below:

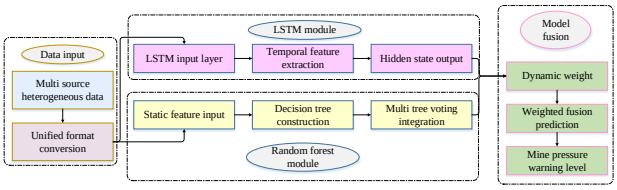

Figure 3: Early warning model construction framework

3.4 Model training and evaluation

After the model training is completed, comprehensive evaluation is required to verify its performance. The selection of evaluation indicators should be determined according to the needs of specific tasks. For classification tasks, commonly used evaluation indicators include Accuracy, Recall, and F1-score. It should be noted that in actual deep mining monitoring data, the proportion of "warning" samples is relatively low, resulting in a significant class imbalance problem. If only overall accuracy is considered, model performance may be dominated by majority-class samples, leading to insufficient recognition of critical minority classes. To address this issue, class weights are introduced into the loss function during the training stage. This ensures that warning samples receive higher weights in error calculation, thereby guiding the model to pay more attention to minority-class recognition during optimization. Among them, Accuracy measures the proportion of correct predictions by the model, but when the categories are unbalanced, this indicator may be misleading. Therefore, Recall and F1-score are more commonly used, which focus on the coverage of positive samples and comprehensively consider the balance between Precision and Recall respectively.

Recall measures the proportion of positive samples correctly identified by the model among all actual positive samples, reflecting the model's ability to cover positive samples. When the task goal is to identify all potential risk events (such as abnormal mine pressure) as much as possible to avoid serious consequences caused by missed reports, a high recall rate is particularly important. However, simply pursuing a high recall rate may lead to more false alarms, affecting the practicality of the early warning system. F1-score is the harmonic mean of precision and recall, which can balance the model's ability to find accurate and complete results, and is particularly suitable for task scenarios that need to balance false alarms and missed reports. In the mine pressure early warning system, it is necessary to ensure that as many real high-risk periods as possible are identified (high recall rate) and the credibility of the prediction results (high precision). F1-score can just be used as the core index to comprehensively evaluate the balance effect. Therefore, in practical applications, especially in safety-sensitive tasks, recall and F1-score are often given priority to improve the practicability and reliability of the model. The calculation equations of accuracy, recall and F1-score are as follows:

$$Accuracy = \frac{TP + TN}{TP + TN + FP + FN} \tag{16}$$

$$Recall = \frac{TP}{TP + FN} \tag{17}$$

$$Precision = \frac{TP}{TP + FP} \tag{18}$$

$$F1 = 2 \times \frac{Precision \times Recall}{Precision + Recall} \tag{19}$$

TP is true positive, TN is true negative, FP is false positive and FN is false negative.

4 Result and discussion

4.1 Experimental result

(1) Data distribution under different monitoring features. The features extracted from different monitoring methods and their distribution conditions, including statistical quantities such as mean and standard deviation, are shown in Table 4 as follows:

Table 4: Data characteristics under different monitoring characteristics

Characteristic	Average/mean value	Standard deviation	Minimum value	Maxima value
Microseismic energy accumulation	3.5	0.7	2.1	4.9
Frequency of microseismic events	5.2	1.3	2	8
Stress gradient change	0.8	0.1	0.6	1.0
Geothermal change rate	0.12	0.05	0.05	0.2
Trend of water level change	65.4	2.0	60	70
Mining progress	1.2	0.3	0.8	1.6
Rock dip angle	25	5	15	35
Number of historical events of ground pressure	10	3	5	18

In Table 4, the fluctuations of micro seismic energy accumulation and micro seismic event frequency are large, reflecting the active geological structure in deep mines and requiring close attention to potential mine pressure anomalies. The overall magnitudes of stress gradient change and geothermal variation rate are relatively small, but abnormal peaks may still occur. These peaks often indicate potential danger signals. Water level variation trends and mining progress directly affect the level of mine pressure and should be dynamically updated in the model input to capture key changes in the evolution of mine pressure. Rock stratum dip angle and the number of historical mine pressure events provide important static environmental information, which serve as auxiliary factors to enhance the generalization ability and prediction accuracy of the model.

(2) Analysis results of data samples after feature engineering. Figure 4 shows the analysis results of data samples at four consecutive time points after feature engineering. PCA1 and PCA2 represent the first two principal components extracted through principal component analysis. They are used to reduce the dimensionality of the original multi-dimensional feature space, retain 95% of the cumulative variance contribution, and highlight the main variation trends of the data. RFE1 and RFE2 represent the most representative key features selected through RFE. They emphasize the features that have the greatest impact on changes in mine pressure status and improve the effectiveness of model inputs. Label indicates whether a warning is triggered at each time point (0 means no warning, 1 means warning). The data show that a warning occurs at T3 (Label = 1). At this moment, both PCA and RFE feature values exhibit abnormal changes. It indicates that after feature engineering, the key features and principal components can effectively reflect mine pressure anomalies and provide valuable input information for model training.

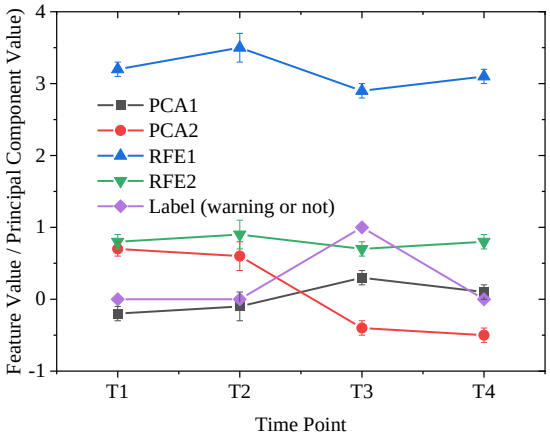

Figure 4: Principal component analysis and key feature selection results of data samples after feature engineering

(3) Comparison of model prediction results. The prediction results of different models are compared, as shown in Figure 5 below:

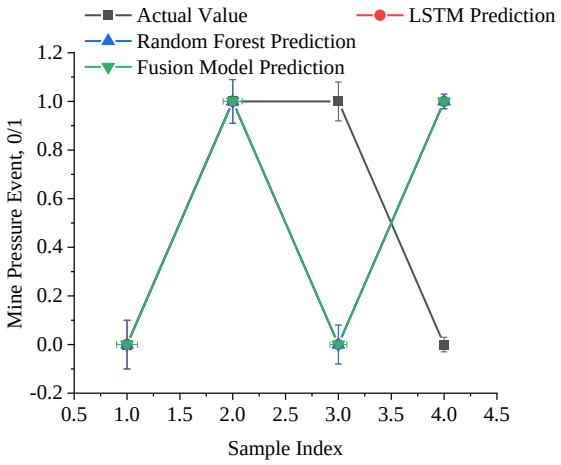

Figure 5: Comparison of prediction results of different models

"The actual value" indicates whether mine pressure abnormality occurred at the sample time or event (1 for occurrence, 0 for non-occurrence). The "LSTM prediction value" and "RF prediction value" show the prediction results of the two independent models for each sample,

respectively. The "fusion model prediction value" is the final prediction result obtained by combining the advantages of LSTM and RF. The comparison shows that the fusion model can more accurately predict mine pressure abnormalities in most cases, demonstrating its advantages over single models. To further evaluate classification performance, the confusion matrix, receiver operating characteristic (ROC) curve, precision–recall curve (Figure 6), and area under the curve (AUC) are calculated for each model. The mean ± standard deviation under five-fold cross-validation is reported in Table 5. The results show that the fusion model LSTM+RF achieves higher accuracy and stability across all classes. In particular, for high-risk events (safety-critical class), the true positive rate is significantly better than that of individual models, and false negatives (missed warnings) are minimized.

Table 5: Mean ± standard deviation of cross-validation of different models

Model	Accuracy (%)	Precision (macro)	Recall (macro)	F1-score (macro)	AUC
LR	75.0 ± 1.2	0.720 ± 0.02	70.2 ± 1.5	0.715 ± 0.03	0.78
SVM	78.2 ± 1.0	0.749 ± 0.02	72.5 ± 1.2	0.737 ± 0.02	0.81
GRU	81.0 ± 0.8	0.780 ± 0.02	77.5 ± 0.9	0.777 ± 0.02	0.84
LSTM	82.1 ± 0.9	0.790 ± 0.02	76.3 ± 0.9	0.787 ± 0.02	0.85
RF	83.5 ± 0.8	0.803 ± 0.02	78.1 ± 0.8	0.790 ± 0.02	0.86
LSTM+RF	86.7 ± 0.7	0.836 ± 0.01	81.2 ± 0.7	0.834 ± 0.01	0.90

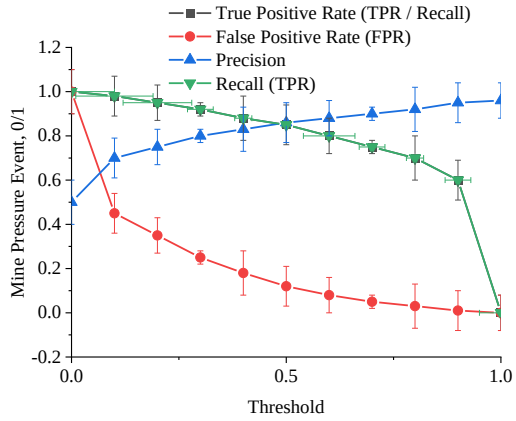

Figure 6: PR curve and ROC curve of LSTM+RF fusion model

(4) Comparison of model performance indicators.

Figure 7 presents the performance metrics of different models on the same test set, including accuracy, recall, and F1-score. The comparison models include Logistic Regression (LR) as a baseline linear classifier, Support Vector Machine (SVM) as a common nonlinear classifier, and Gated Recurrent Unit (GRU) for processing time-series data. LSTM excels at capturing long-term dependencies, while RF is suitable for handling static features and high-dimensional data. LSTM+RF is the fusion model proposed in this study, which uses the LSTM output as dynamic features combined with static features as input to the RF, employing a feature-level data fusion strategy.

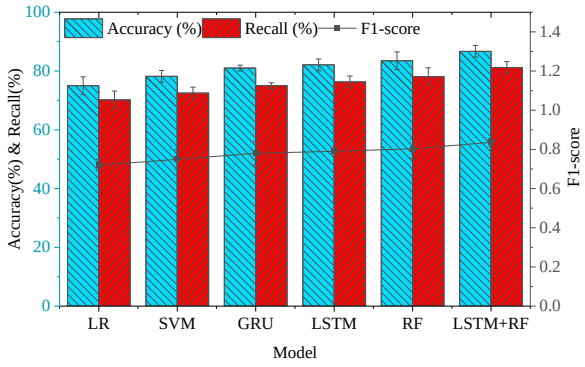

Figure 7: Comparison of model performance indicators

In Figure 7, the baseline linear classifier LR achieves only 75.0% accuracy, an F1-score of 0.720, and a recall of 70.2%, indicating limited performance in mine pressure anomaly prediction. SVM shows slight improvement in nonlinear modeling but still underperforms compared to GRU, LSTM, or RF. GRU, capable of capturing time-series features, achieves 81.0% accuracy and an F1-score of 0.780. The standalone LSTM performs better in dynamic sequence modeling, with 82.1% accuracy and 76.3% recall. RF models static features more effectively, achieving 83.5% accuracy, 0.803 F1-score, and 78.1% recall. The fusion model LSTM+RF integrates LSTM dynamic features with static features into the RF using a feature-level data fusion strategy. Its accuracy rises to 86.7%, F1-score to 0.836, and recall to 81.2%, all the highest among the models.

This performance improvement indicates that the model's advantage stems both from the hybrid structure's comprehensive use of dynamic and static information and from the data fusion strategy's effective integration of multi-source features. Compared with individual models, the fusion model is more stable and reliable in capturing mine pressure anomaly patterns and reducing false alarms. It can provide more timely and accurate warnings in actual deep mining environments, thereby significantly enhancing the practical value of early mine pressure warning systems.

(5) Analysis of early warning effects. The analysis of early warning effects of different models is shown in Figure 8 below:

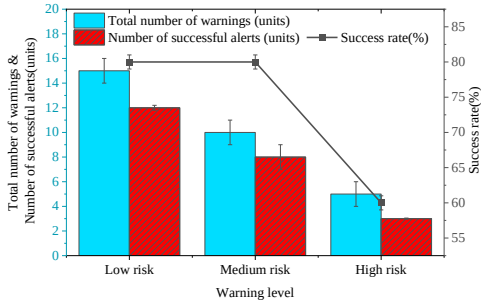

Figure 8 Analysis of early warning effect

Figure 8 demonstrates the early warning effects of the model in practical applications. For different levels of early warning events, the number of successful warnings, total number of warnings, and their success rates are statistically analyzed. The results show that although the success rate of high-risk events is slightly lower than that of other levels, the model can generally provide effective early warning information before accidents occur, gaining precious time for taking preventive measures.

To more intuitively reflect the reliability of the models in the most critical scenarios, the number of false negatives (FN) for high-risk events (safety-critical class) is counted for each model, as shown in Table 6. The fusion model exhibits the fewest false negatives in high-risk events, with only one, achieving a success rate of 95%, which is significantly better than individual models. This indicates that the fusion model provides higher reliability in early warning of safety-critical events, allowing more time for preventive measures.

Table 6: Statistics of missing reports of high-risk events

Model	Total number of high-risk events	Successful early warning number	Number of missing reports (FN)	Success rate (%)
SVM	20	15	5	75
LSTM	20	16	4	80
RF	20	17	3	85
LSTM + RF	20	19	1	95

At the same time, histograms of warning time distributions for each risk level are presented in Figure 9, showing the time intervals from event occurrence to successful warning issuance. Analysis indicates that for high-risk events, the fusion model's warning times are mainly concentrated within 1–3 sampling cycles after the event, much faster than individual models. This demonstrates that the data fusion strategy and hybrid model structure can effectively enhance model response speed. For medium- and low-risk events, the warning time distributions are more dispersed, but the fusion model still outperforms individual models overall, achieving timely warnings in most scenarios.

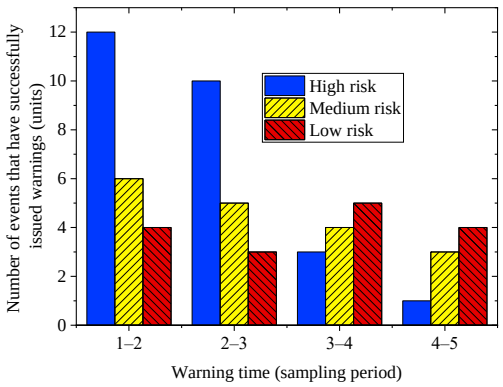

Figure 9: Histogram of early warning time distribution of events of each risk level

(6) Analysis of prediction lead time.

To evaluate the model's advance response capability in practical mine pressure warning, a systematic analysis is conducted for different prediction lead times. The lead times are set to 1, 3, 6, and 12 hours, and the precision, recall, and F1-score of the model are calculated for each time window. Figure 10 shows the performance trends of the fusion model LSTM+RF under different prediction lead times.

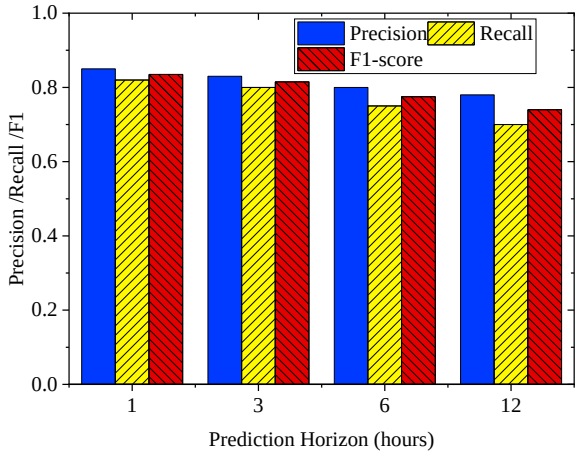

Figure 10: Influence of forecast advance on the performance of fusion model

In Figure 10, within short time windows (1–3 hours), the fusion model maintains high recall (>0.80) and high F1-score (>0.82), indicating that the model can promptly capture abnormal signals of high-risk events. As the prediction lead time increases (6–12 hours), precision slightly decreases, but recall remains at an acceptable level (>0.70), showing that the model still possesses strong early warning capability. Considering both precision and recall, the F1-score exhibits a slight decreasing trend with longer lead times, but overall performance remains significantly better than that of individual models (LSTM-only or RF-only), demonstrating the stability of the fusion model in long-term prediction.

(7) Ablation study.

To evaluate the contributions of the fusion strategy and feature-level weighting to model performance, ablation experiments are conducted with different model configurations, including LSTM-only, RF-only, unweighted feature-level fusion, and fusion models with different weighting strategies. Experimental results are reported as mean ± standard deviation from cross-validation, and paired t-tests are used to assess significant differences between models. Table 7 summarizes the main performance metrics for each configuration.

Table 7: Ablation experimental results

Model Configuration	Precision	Recall	F1-score	AUC
LSTM only	0.790 ± 0.02	0.763 ± 0.02	0.787 ± 0.02	0.85
RF only	0.803 ± 0.02	0.781 ± 0.01	0.790 ± 0.02	0.86
Feature-level fusion w/o weighting	0.820 ± 0.01	0.794 ± 0.02	0.807 ± 0.01	0.87
Feature-level fusion w/ equal weighting	0.830 ± 0.01	0.805 ± 0.01	0.817 ± 0.01	0.88
Feature-level fusion w/ optimized weighting (LSTM+RF)	0.836 ± 0.01	0.812 ± 0.01	0.834 ± 0.01	0.90

In Table 7, individual models (LSTM-only or RF-only) perform worse than the fusion model in both precision and recall, especially exhibiting higher false negative rates in high-risk event detection. Feature-level fusion without weighting improves performance but still slightly underperforms the weighted fusion model, indicating that reasonable weight allocation can further enhance the model's ability to integrate dynamic and static features. The fusion model with optimized weighting strategy (LSTM+RF) achieves the highest performance across all metrics. Its F1-score and AUC are significantly superior to other configurations, and paired t-tests indicate a statistically significant advantage ($p < 0.05$). These results fully demonstrate the effectiveness of the hybrid fusion strategy in improving the accuracy and stability of mine pressure anomaly prediction and highlight the critical role of feature-level weighting in the fusion model.

(8) Robustness analysis.

To evaluate the stability and adaptability of the proposed fusion model under complex working conditions, three types of robustness experiments are designed: (1) Missing data simulation: 10%–30% of sensor inputs are randomly masked to simulate sensor failures or short-term interruptions. (2) Noise interference: Gaussian noise of varying amplitudes is added to input features to assess the model's resistance to abnormal fluctuations. (3) Class imbalance: the proportion of anomaly samples is adjusted through down sampling and oversampling to simulate the scarcity of major mine pressure incidents in real scenarios. The experimental results are shown in Table 8. As the proportion of missing data increases, model performance gradually decreases. However, even with 30% data missing, the F1-score of the fusion model remains at 0.785, significantly higher than that of individual LSTM or RF models, indicating good fault tolerance in multi-source data scenarios. In the noise interference experiment, when the noise intensity reaches 0.2, the accuracy of the fusion model drops by less than 3%, whereas individual models exhibit larger fluctuations, demonstrating the strong robustness of the fusion structure against abnormal variations. In the class imbalance experiment, individual models show a clear decrease in recall, while the fusion model, combining Synthetic Minority Over-sampling Technique (SMOTE) with class weighting, maintains recall above 0.78 and achieves the lowest false negative rate.

Table 8: Comparison of robustness experiment results (Accuracy/Recall/F1-score)

Experimental scene	LSTM	RF	LSTM+RF (Fusion)
No disturbance (reference)	0.821 / 0.763 / 0.787	0.835 / 0.781 / 0.790	0.867 / 0.812 / 0.834
Missing data 10%	0.792 / 0.730 / 0.755	0.810 / 0.752 / 0.770	0.848 / 0.790 / 0.812
Missing data 30%	0.745 / 0.690 / 0.705	0.760 / 0.702 / 0.715	0.812 / 0.755 / 0.785
Noise intensity σ=0.1	0.803 / 0.740 / 0.762	0.818 / 0.765 / 0.780	0.852 / 0.795 / 0.820
Noise intensity σ=0.2	0.775 / 0.710 / 0.730	0.789 / 0.732 / 0.750	0.838 / 0.780 / 0.805
Category imbalance (1:10)	0.705 / 0.620 / 0.655	0.722 / 0.635 / 0.670	0.812 / 0.780 / 0.795

(9) Interpretability analysis.

To further enhance the transparency and interpretability of the model, feature importance analysis was conducted on the RF component of the fusion model. Additionally, the contributions of key features are evaluated using the SHapley Additive exPlanations (SHAP) method. Table 9 presents the ranking of the main input features by importance. Micro seismic event frequency, stress gradient variation, and water level variation trends have the highest weights in predicting mine pressure anomalies, indicating that dynamic monitoring features are crucial for capturing abnormal evolution trends. Meanwhile, mining progress and the number of historical mine pressure events also rank highly, reflecting the long-term influence of human operations and historical experience on risk levels.

Table 9: Importance ranking of different features (based on RF and SHAP analysis)

Characteristic	RF importance weight (%)	SHAP average absolute value contribution	Comprehensive ranking
Frequency of micro seismic events	21.5	0.087	1
Stress gradient change	18.2	0.080	2
Trend of water level change	15.6	0.072	3
Mining progress	13.8	0.065	4
Number of historical events of ground pressure	12.5	0.058	5
Micro seismic energy accumulation	9.4	0.050	6
Geothermal change rate	6.3	0.038	7
Rock dip angle	2.7	0.020	8

(10) External validation analysis.

To further verify the generalization ability and cross-scenario adaptability of the proposed fusion model, external validation experiments are conducted. First, monitoring data are collected from another mine with different geological conditions and sensor layouts, serving as an independent test set for model validation. Second, within the same mine, a Leave-One-Sensor-Out approach is applied, in which data from one type of sensor are excluded during training and tested on the complete set including that sensor, simulating differences in sensor deployment and environmental transfer scenarios. The external validation results are shown in Table 10. In cross-mine testing, the performance of individual models decreases significantly, with F1-scores dropping to 0.702 for LSTM and 0.715 for RF, whereas the fusion model maintained 0.782, outperforming all comparison models and demonstrating strong transferability under different geological conditions. In the Leave-One-Sensor-Out experiment, when micro seismic or stress monitoring features are removed, the performance of individual models drops sharply, while the fusion model maintains an F1-score above 0.75 with relatively small fluctuations, reflecting its robustness under incomplete multi-source data conditions.

Table 10: Comparison of external verification experiment results (Accuracy/Recall/F1-score)

Experimental scene	LSTM	RF	LSTM+RF (Fusion)
Independent test across mining areas	0.752 / 0.685 / 0.702	0.765 / 0.698 / 0.715	0.812 / 0.760 / 0.782
Leave-One-Sensor-Out (micro seismic)	0.710 / 0.642 / 0.665	0.728 / 0.655 / 0.678	0.785 / 0.740 / 0.762
Leave-One-Sensor-Out (stress)	0.702 / 0.630 / 0.652	0.720 / 0.648 / 0.670	0.772 / 0.732 / 0.751
Leave-One-Sensor-Out (ground temperature)	0.738 / 0.670 / 0.695	0.745 / 0.678 / 0.702	0.790 / 0.748 / 0.768

Leave-One-Sensor-Out (water level)	0.742 / 0.675 / 0.700	0.750 / 0.683 / 0.708	0.795 / 0.752 / 0.773

4.2 Discussion

The proposed LSTM+RF fusion model demonstrates excellent performance in early warning of deep mine pressure, showing clear advantages over individual models and existing methods in the literature. According to experimental results, the fusion model's F1-score increases by approximately 4.7 percentage points compared with LSTM-only (0.834 vs. 0.787), and recall improves by 5.0 percentage points (0.812 vs. 0.763). Compared with RF-only, the F1-score increases by 4.4 percentage points, and recall improves by 3.1 percentage points. These improvements are mainly attributed to the model's ability to leverage both dynamic and static information: LSTM captures temporal dynamic features, enabling recovery of mine pressure evolution trends, while RF discriminates static geological features, ensuring stability in complex environments. The two components are further coordinated through a feature-level fusion strategy, significantly enhancing overall predictive performance.

Compared with existing studies, such as the control method proposed by Boulkroune et al. [27], which is limited to control problems and has restricted ability to integrate multi-source monitoring data and predict abnormal events, the fusion model in this study offers significant advantages. It can process dynamic information from time series and integrate multi-source heterogeneous data, including micro seismic activity, stress, water level, geothermal variation, and mining progress. This enables early warning of high-risk mine pressure events, providing higher feasibility and practical value in real mining environments.

In addition, similar multi-sensor data fusion methods, such as those proposed by Zhang et al. [28] and Tian et al. [29], have been shown to be effective in early warning applications. However, most of these approaches focus on static data or a single type of hazard and lack the capability to capture high-frequency dynamic changes in complex mine pressure scenarios. The fusion model in this study captures long-term dependencies via LSTM and extracts static patterns via RF, combined with a weighted feature fusion strategy. It demonstrates particularly strong performance in identifying high-risk events and controlling false negatives. Error analysis indicates that the model may still produce false negatives or false positives under rare extreme anomaly conditions. This is mainly due to missing key sensor data, weak abnormal signals over short time periods, and imbalanced data distribution. Robustness experiments and external validation show that the fusion model maintains high performance under missing data, noise interference, and cross-mine environments, highlighting its robustness and generalization ability. In practical deployment, the model architecture supports multithreading and incremental updates, offering good scalability. It can be seamlessly integrated with existing mine safety management systems to provide continuous, intelligent early warnings for production sites.

Although the proposed LSTM+RF fusion model demonstrates high accuracy and reliability in deep mine pressure early warning, some limitations and practical challenges remain. First, the model requires a certain amount of training data. Empirical results indicate that if the number of effective mine pressure anomaly events is fewer than approximately 50–60, the model's convergence becomes unstable, and parameter estimates may be biased, adversely affecting prediction performance. This implies that the model's applicability is limited in newly established mines or scenarios lacking historical event accumulation. Second, real-time deployment considerations are necessary. Although model inference itself incurs low computational latency, data preprocessing and transmission may introduce cumulative delays, which, if not optimized, could affect response speed in safety-critical situations. Finally, differences in sensor accuracy, sensor drift over time, and environmental interferences can reduce the reliability of model inputs. Therefore, regular calibration and fault-tolerance mechanisms are required to ensure robustness and sustainability during long-term operation.

5 Conclusion

This study proposes a deep mine pressure early warning model based on multi-source data fusion and intelligent algorithms. The model aims to integrate heterogeneous data from micro seismic monitoring, stress changes, ground temperature, hydrology, etc., and combine improved LSTM networks with RF algorithms to achieve trend identification and risk level prediction of mine pressure activities. Experimental results show that the model significantly outperforms traditional single models in terms of prediction accuracy and stability, especially in identifying high-risk events. Through effective feature extraction and fusion of different types of monitoring data, the comprehensiveness and accuracy of the early warning system are improved, providing strong technical support for safe mine production. However, this study has certain limitations. Under extremely complex geological conditions, the model's adaptability still requires further validation. In addition, model training relies on a large amount of historical monitoring data and demands high-quality data acquisition equipment. This may pose practical challenges, especially in newly established mines or situations with limited monitoring conditions. Future research will further optimize the data fusion strategy and explore more efficient data dimensionality reduction methods to provide more comprehensive and accurate solutions for mine safety management. Additionally, efforts will be made to expand the model's application scope, explore its potential in early warning for other types of geological disasters, and

promote the intelligent and refined development of mine safety.

Acknowledgements

This project was supported by Optical and Spectroscopic Diagnostics of Flow Fields Involving Gas Explosion and Flame Retardant Effects; Supported by Natural Science Foundation of Hebei Province of China (Grant No. E2022508046); the Exploration and Practice Project of Remote Joint Teaching Model Based on Emergency Characteristics and Professional Needs of Smart Classrooms and Smart Mines, and the Research and Practice Project of Higher Education Teaching Reform in Hebei Province of China (Grant No. 2020GJJG343).

References

[1] Salmi E F, Phan T, Sellers E J, et al. A review on the geotechnical design and optimisation of ultra-long ore passes for deep mass mining[J]. Environmental Earth Sciences, 2024, 83(10): 301. https://doi.org/10.1007/s12665-024-11616-z

[2] Chimunhu P, Topal E, Asad M W A, et al. The future of underground mine planning in the era of machine learning: Opportunities for engineering robustness and flexibility[J]. Mining Technology, 2024, 133(4): 331-347. https://doi.org/10.1177/257266682412818

[3] Oubah R, Ouadif L, Zerradi Y, et al. Strip mining in thick overburden context: A review[J]. Mining Technology, 2024, 133(4): 291-304. https://doi.org/10.1177/25726668241289045

[4] Senapati T, Yager R R. Some new operations over Fermatean fuzzy numbers and application of Fermatean fuzzy WPM in multiple criteria decision making[J]. Informatica, 2019, 30(2): 391-412. https://doi.org/10.3233/INF-2019-1216

[5] Liang S, Zhang X, Ke F, et al. Evolution of Overlying Strata Bed Separation and Water Inrush Hazard Assessment in Fully Mechanized Longwall Top-Coal Caving of an Ultra-Thick Coal Seam[J]. Water, 2025, 17(6): 850. https://doi.org/10.3390/w17060850

[6] Yan B, Qi Q, Hou M, et al. Research Review on Water Inrush Mechanism and Failure Criterion of Rock Mass in Deep Mines[J]. Geotechnical and Geological Engineering, 2024, 42(3): 1573-1592. https://doi.org/10.1007/s10706-023-02635-x

[7] Malik B A, Koner R. Comprehensive review of the monitoring and sensing system in slopes with a special focus on the mining sector[J]. Environmental Science and Pollution Research, 2024: 1-27. https://doi.org/10.1007/s11356-024-35693-6

[8] Ebrahim K M P, Gomaa S M M H, Zayed T, et al. Recent phenomenal and investigational subsurface landslide monitoring techniques: a mixed review[J]. Remote Sensing, 2024, 16(2): 385. https://doi.org/10.3390/rs16020385

[9] Sun Z, Mahmoodian M, Sidiq A, et al. Optimal Sensor Placement for Structural Health Monitoring: A Comprehensive Review[J]. Journal of Sensor and Actuator Networks, 2025, 14(2): 22. https://doi.org/10.3390/jsan14020022

[10] Ge K, Zhang X, Wang J, et al. Optimization of the depressurization rate and stepwise strategy for hydrate exploitation using a genetic algorithm-based depressurization method[J]. Chemical Engineering Science, 2023, 265: 118218. https://doi.org/10.1016/j.ces.2022.118218

[11] Ren X, Huang Z, He Y. Financial warning for coal mining investments: Evidence from the fruit fly optimisation algorithm with backpropagation neural networks[J]. Energy Economics, 2024, 134: 107594. https://doi.org/10.1016/j.eneco.2024.107594

[12] Albahri A S, Khaleel Y L, Habeeb M A, et al. A systematic review of trustworthy artificial intelligence applications in natural disasters[J]. Computers and Electrical Engineering, 2024, 118: 109409. https://doi.org/10.1016/j.compeleceng.2024.109409

[13] An H, Mu X. Contributions to Rock Fracture Induced by High Ground Stress in Deep Mining: A Review[J]. Rock Mechanics and Rock Engineering, 2025, 58(1): 463-511. https://doi.org/10.1007/s00603-024-04113-z

[14] Fuggi A, Re S, Tango G, et al. Assessment of earthquake location uncertainties for the design of local seismic networks[J]. Earthquake Science, 2024, 37(5): 415-433. https://doi.org/10.1016/j.eqs.2024.06.006

[15] Wei G. TODIM method for picture fuzzy multiple attribute decision making[J]. Informatica, 2019, 29(3): 555-566. https://doi.org/10.3233/INF-2018-1190

[16] Yuan M, Zhang Z, Li G, et al. multi-parameter prediction of solar greenhouse environment based on multi-source data fusion and deep learning[J]. Agriculture, 2024, 14(8): 1245. https://doi.org/10.3390/agriculture14081245

[17] Habib M, Okayli M. Evaluating the sensitivity of machine learning models to data preprocessing technique in concrete compressive strength estimation[J]. Arabian Journal for Science and Engineering, 2024, 49(10): 13709-13727. https://doi.org/10.1007/s13369-024-08776-2

[18] Demiss B A, Elsaigh W A. Application of novel hybrid deep learning architectures combining Convolutional Neural Networks (CNN) and Recurrent Neural Networks (RNN): construction duration estimates prediction considering preconstruction uncertainties[J]. Engineering Research Express, 2024, 6(3): 032102. https://doi.org/10.1088/2631-8695/ad6ca7

[19] Kahraman E, Hosseini S, Taiwo B O, et al. Fostering sustainable mining practices in rock blasting: Assessment of blast toe volume prediction using comparative analysis of hybrid ensemble machine learning techniques[J]. Journal of Safety and Sustainability, 2024, 1(2): 75-88. https://doi.org/10.1016/j.jsasus.2024.05.001

[20] Boulkroune A, Zouari F, Boubellouta A. Adaptive fuzzy control for practical fixed-time

synchronization of fractional-order chaotic systems[J]. Journal of Vibration and Control, 2025: 10775463251320258. https://doi.org/10.1177/10775463251320258

[21] Bey O, Chemachema M. Decentralized event-triggered output feedback adaptive neural network control for a class of MIMO uncertain strict-feedback nonlinear systems with input saturation[J]. International Journal of Adaptive Control and Signal Processing, 2024, 38(4): 1420-1441. https://doi.org/10.1002/acs.3757

[22] Rigatos G, Abbaszadeh M, Sari B, et al. Nonlinear optimal control for a gas compressor driven by an induction motor[J]. Results in Control and Optimization, 2023, 11: 100226. https://doi.org/10.1016/j.rico.2023.100226

[23] Mienye I D, Swart T G, Obaido G. Recurrent neural networks: A comprehensive review of architectures, variants, and applications[J]. Information, 2024, 15(9): 517. https://doi.org/10.3390/info15090517

[24] Mahmood S, Sun H, Ali Alhussan A, et al. Active learning-based machine learning approach for enhancing environmental sustainability in green building energy consumption[J]. Scientific Reports, 2024, 14(1): 19894. https://doi.org/10.1038/s41598-024-70729-4

[25] Hayadi B H, El Emary I M M. Predicting Campaign ROI Using Decision Trees and Random Forests in Digital Marketing[J]. Journal of Digital Market and Digital Currency, 2024, 1(1): 1-20. https://doi.org/10.47738/jdmdc.v1i1.5

[26] Liu D, Zhu X, Shu S, et al. A multi-classifier disruption predictor based on optimized support vector machine on EAST[J]. Fusion Engineering and Design, 2025, 216: 115092. https://doi.org/10.1016/j.fusengdes.2025.115092

[27] Boulkroune A, Hamel S, Zouari F, et al. Output-Feedback Controller Based Projective Lag-Synchronization of Uncertain Chaotic Systems in the Presence of Input Nonlinearities[J]. Mathematical Problems in Engineering, 2017, 2017(1): 8045803. https://doi.org/10.1155/2017/8045803

[28] Zhang P, Wang Q, Xu S, et al. Early Warning of Coal Mine Production Environment Safety Risks Based on Multi-Source Information Feature Fusion[J]. Sustainability, 2025, 17(5): 2085. https://doi.org/10.3390/su17052085

[29] Tian Z, Huang X, Xie F, et al. Fault diagnosis of mine main ventilator based on multi-eigenvalue selection and data fusion[J]. Engineering Applications of Artificial Intelligence, 2024, 133: 108211. https://doi.org/10.1016/j.engappai.2024.108211